npj Heritage Science

https://doi.org/10.1038/s40494-026-02568-7

Article in Press

Deciphering 4000-year-old cuneiform letters hidden in clay envelopes using a mobile X-ray computed tomography scanner

Received: 17 February 2026

Accepted: 13 April 2026

Cite this article as: Michel, C., Schroer, C.G., Olbrich, S. *et al.* Deciphering 4000-year-old cuneiform letters hidden in clay envelopes using a mobile X-ray computed tomography scanner. *npj Herit. Sci.* (2026). https://doi.org/10.1038/s40494-026-02568-7

Cécile Michel, Christian G. Schroer, Stephan Olbrich, Andreas Beckert, Samaneh Ehteram, Andreas Schropp, Philipp Paetzold, Ralph Döhrmann, Patrik Wiljes, Stephan Botta, Mathias Bohn, Katrin Zerbe & Avni Aksoy

Deciphering 4,000-year-old cuneiform letters hidden in clay envelopes using a mobile X-ray computed tomography scanner

Cécile Michel[1,2*†], Christian G. Schroer[2,3,4*†], Stephan Olbrich[2], Andreas Beckert[2], Samaneh Ehteram[2], Andreas Schropp[2,3*], Philipp Paetzold[3], Ralph Döhrmann[3], Patrik Wiljes[3], Stephan Botta[3], Mathias Bohn[3], Katrin Zerbe[3], Avni Aksoy[5]

[1*]ArScAn-HASAÉ, CNRS, Maison des Sciences de l'Homme Mondes, bât. René-Ginouvès, 21, allée de l'Université, F-92023 Nanterre Cedex, France.

[2]Centre for the Study of Manuscript Cultures (CSMC), University of Hamburg, Warburgstraße 26, D-20354 Hamburg, Germany.

[3]Centre for X-ray and Nano-Science (CXNS), Deutsches Elektronen-Synchrotron (DESY), Notkestraße 85, D-22607 Hamburg, Germany.

[4]Helmholtz Imaging, Deutsches Elektronen-Synchrotron (DESY), Notkestraße 85, D-22607 Hamburg, Germany.

[5]Deutsches Elektronen-Synchrotron DESY, Zeuthen, Germany.

*Corresponding author(s). E-mail(s): cecile.michel@cnrs.fr; christian.schroer@desy.de; andreas.schropp@desy.de;
Contributing authors: stephan.olbrich@uni-hamburg.de; andreas.beckert@uni-hamburg.de; samaneh.ehteram@desy.de; philipp.paetzold@desy.de; ralph.doehrmann@desy.de; patrik.wiljes@desy.de; stephan.botta@desy.de; mathias.bohn@desy.de; katrin.zerbe@desy.de; avni.aksoy@desy.de;

†These authors contributed equally to this work.

Abstract

Hundreds of cuneiform clay tablets unearthed in South-western Asia remain sealed within clay envelopes, leaving their texts inaccessible to Assyriologists.

Computed tomography (CT) enables to look inside the clay envelopes non-destructively. An interdisciplinary team developed a transportable high-definition CT scanner named by ENCI, designed for on-site use in museums and archives. ENCI allows researchers to visualise the cuneiform text written on hidden tablets, study clay inclusions, and analyse manufacturing techniques without opening the tablets. First deployed at the Louvre Museum in Paris in 2024, it was later used at the Museum of Anatolian Civilisations in Ankara to scan around fifty encased tablets, many of them letters. Combined with advanced 3D surface extraction and visualisation software, ENCI enables virtual unwrapping and detailed exploration of small objects. This technology opens new possibilities for studying cultural heritage artefacts on site, while also revealing mineral and organic inclusions and evidence of envelope formation methods.

Introduction

Between half a million and a million of cuneiform artefacts have been uncovered in South-Western Asia, especially in Iraq, Syria, Iran, and Türkiye. These texts, written in a dozen different languages, document the first two-thirds of the recorded human history, from 3400 BCE to 200 CE. Among the many different types of texts found, those written for utilitarian purposes from the second half of the third millennium onwards were sometimes enclosed in a clay envelope bearing only a few lines of text and several seal impressions on the outside [1, 2].

This is the case for legal and administrative texts as well as for letters. The sealed envelope of legal tablets certified the validity of the document as long as the envelope remained intact. The text or a summary of it was copied onto the envelope in order to understand what was at stake. Once the contract was completed, the envelope was broken and the text no longer had any legal value. The same applied occasionally for administrative tablets.

Letters, especially during the first half of the second millennium BCE, were enclosed in a clay envelope on which only the names of the sender and addressee were written, and the sender's cylinder seal was rolled. A legendary text explains the main reason for the invention of the envelope. King Ur-Zababa of Kish, who would have reigned around 2340 BCE, wanted to send to death the messenger carrying the letter containing instructions to kill him without the latter knowing it: *In those days, although writing words on tablets existed, putting tablets into envelopes did not yet exist. King Ur-Zababa dispatched Sargon, the creature of the gods, to Lugal-zagesi in Uruk with a message written on clay, which was about murdering Sargon* [3, lines 53-56]. The envelope was thus invented to protect the confidentiality of the text. Letter envelopes also protected the clay tablet during transport, and authenticated the sender who rolled his cylinder seal on the surface of the clay.

Making envelopes required a certain amount of skill to obtain a thin layer of clay and fit it around the tablet without it sticking to it. Clay shrinks as it dries, so an envelope that fit too snugly would break after a few hours, while on an envelope that was too loose it would be impossible to write or roll one's seal. As the clay envelope

dries, it follows the contours of the tablet to such an extent that the cuneiform signs printed in negative on the tablet are reproduced in positive on the inside of the envelope [2]. The layer of air separating the surface of the tablet from that of the envelope is extremely thin, and sometimes non-existent.

The recipient had to break the envelope to read the letter, thus envelopes should be exceptional. However, many fragments of envelopes have been found, either because envelopes were opened in ancient times and fragments were not removed from the archives, or, more likely, because envelopes were broken when buildings collapsed. The discovery of intact envelopes with their tablet inside can only be explained if the letter never reached its addressee: either it was never sent or never delivered for other reasons.

Several hundreds of contract and letter envelopes were found still intact in the houses of Assyrian merchants who settled at Kültepe, ancient Kanesh, in central Anatolia, during the 19th and 18th centuries BCE. A thousand kilometres away from their home city Assur in Northern Iraq, they received many letters from their family members and colleagues that they archived together with other documents. Most of these cuneiform artefacts are now preserved in the Museum of Anatolian Civilisations in Ankara, Türkiye.

In the last century, a small selection of sealed envelopes was opened to allow Assyriologists to access the tablet's hidden text. This irreparably damaged the miniature scenes of the seal impressions, preventing any study. For several decades now, the clay envelopes are no longer opened, and new techniques have to be implemented to enable the hidden text to be read.

Computed tomography allows the visualisation of the internal structure of objects, giving access to the surface of the encased tablet. However, museums are only rarely equipped with such large and expensive instruments, the British Museum being an exception [4]. As part of an interdisciplinary research project, we have designed and built a transportable high-definition scanner for X-ray computed tomography — ENCI, for Extracting Non-destructively Cuneiform Inscriptions. When combined with surface extraction and rendering, tomograms reveal the cuneiform texts written on encased tablets, as well as inclusions in the clay of the tablets and envelopes, and the techniques used to produce them [5]. ENCI was first tested on contracts at the Louvre Museum in Paris in February 2024, before being taken to the Museum of Anatolian Civilisations in Ankara in September and October 2024 to investigate around fifty encased letters and contracts. The main results of this project, including the tomographic data acquisition and processing, their visualisation in 3D, as well as the deciphering of the cuneiform writings and their interpretation, are presented here.

Methods

ENCI, a high-resolution and transportable CT scanner

Tools to analyse and visualise cuneiform tablets have been developed for more than two decades, primarily based on geometric data such as triangulated representation of its surface [6–9], which were typically acquired by surface scanning techniques. These 3D scanning methods are limited to digitising the exterior of artefacts. X-ray computed

tomography (CT) has been shown to be well suited to the study of cuneiform clay tablets and reveal their inner structure in 3D. For example, Old Assyrian contracts from the Böhl collection at the Netherlands Institute for the Near East (NINO) in Leiden were scanned in a micro-CT scanner at the Faculty of Civil Engineering and Geosciences (CEG) at TU Delft in the Netherlands, revealing the hidden text on the enclosed cuneiform tablets [10, 11].[1] While some museums, such as the British Museum in London, have modern micro-CT systems well-suited for detailed studies of cuneiform clay tablets [4], most museums lack the means to record CT images of their artefacts on site. For those museums that have 2D X-ray imaging capabilities on site, Bossema et al. [13] have shown a way to upgrade their 2D imaging systems to 3D CT at a low investment cost. However, this approach requires a radiation safe environment and fairly sophisticated data analysis. In most cases, museums do not have access to X-ray analytics on site.

In addition, museums do not usually make their artefacts available for study outside of their premises. In this case, cuneiform tablets can only be read in or very close to the museum's archives. At the Museum of Anatolian Civilisations in Ankara, for example, the artefacts can only be studied at a few workbenches in the corridor outside the archive, accessible only by a narrow staircase. As a result, the X-ray tomography scanner has to be brought into the museum and carried up the stairs. It has to be operable as a full protection device in public space without any additional safety requirements. Commercial micro-CT scanners are typically quite heavy[2] and transportable only with considerable effort. None of these systems could be practically used in the field and in the large important collections.

We therefore decided to design and build a portable micro-CT scanner with full radiation protection, optimised for the study of cuneiform clay tablets. The main objective was to image clay tablets up to a size of 100 mm × 50 mm × 200 mm with a spatial resolution better than 50 µm in order to clearly resolve the writing, see enough detail to distinguish between the handwriting of different scribes, and resolve the very small air gap between the tablet and the envelope. As archive opening hours are usually very limited, the data acquisition needs to be as fast as possible to enable a significant number of tablets to be scanned in a working day. Computing and controls should be powerful enough to allow for continuous data acquisition and parallel tomographic reconstruction for fast feedback during the experimental campaign. The system is designed to be self-contained and not dependent on an internet connection. It should not require more power than is available from a 230 V wall socket.

Penetrating clay objects of the given dimensions requires high-energy X-rays well above 100 keV. As a result, we chose an X-ray tube with acceleration voltage up to 180 kV. For the scanner to provide full protection, the radiation dose rate in its vicinity must never exceed 0.5 µSv h^{-1} to stay below the effective dose limit of 1 mSv to which the general public is typically exposed over the course of a year from all other external sources. These requirements entail the technical design described below.

[1] X-rays are also well suited to obtain chemical or structural information from the clay using fluorescence analysis [12] and diffraction.

[2] The Phoenix Nanotom M from Baker Hughes [14] used in the study at the CEG at TU Delft [10] has a mass of almost two tonnes, while other systems, such as the TESCAN UniTom XL also used at the institute, reach up to 6.5 t [15].

Many museums and archives do not provide a fast and reliable internet connection. Therefore, the system is required to be able to store the data from a full experimental campaign and to run the full data processing pipeline offline and in parallel with data acquisition in order to support near-real-time exploration of cuneiform tablets on site.

Technical Design

Fulfilling the scientific requirements described in the previous section implies strict and in some ways contradicting technical requirements. To achieve the radiation protection at the given X-ray energies, considerable shielding is required, which adds significantly to the weight of the instrument. To keep it portable, we applied the following design rules: 1) keep the surface area of the shielded volume as small as possible, 2) optimise the shielding thickness for the local radiation levels, and 3) make the system modular so that individual components can be carried separately.

These three design rules have an impact on the overall design: Rule 1 implies that the optical path must be rather short. This makes the imaging geometry highly conical. Rule 2 requires detailed modelling of the radiation to maintain a constant safety margin for all shielding components while keeping them as light as possible. Rule 3 requires a modular design with tight fits for all components to prevent radiation leakage. In addition, the safety interlock must be designed to ensure that all components are correctly assembled before the X-rays can be switched on.

Based on these design rules, the scanner was designed and built in about four years at the DESY research centre in Hamburg, Germany. In Fig. 1a the modular design is shown. The scanner can be disassembled into 8 components that can be handled separately during transport. Most of these components have a mass of about 50 kg and can be handled by two people. The server rack (component 8 in Fig. 1a), which contains all the control and supply units and the storage and computing units, weighs about 100 kg and is typically handled by four people. The total assembly weighs about 420 kg. The system can be assembled on site and taken into operation in about two hours, including calibration of the imaging geometry and all safety checks.

Figs. 1b and 1c show the instrument at the Museum of Anatolian Civilisations in Ankara, Türkiye. Table 1 summarises the most important parameters of the scanner.

Radiation protection, controlling and data storage

ENCI has CE certification and radiation protection approval within the scope of the German Radiation Protection Act. After notification to the local radiation protection authority, it can be operated anywhere in Germany as a portable device. Radiation approval in other countries must be applied for separately in each country. For Türkiye, ENCI has full radiation protection approval for mobile operations for the next five years.

Computing and controls are implemented in the server rack (component 8 in Fig. 1a). The system uses the Tango device server / Sardana controls client concept commonly used for experimental control at synchrotron radiation sources. The data structure is fully compatible with dCache [16] used for scientific data storage at DESY.

Table 1 Specifications and parameters of the tomographic scanner ENCI.

source: Finetec FOMM 180.01S TT	
acceleration voltage	up to 180 kV
maximal power	80 W
source size	
smallest	5 µm
at 80 W	25 µm
target material	tungsten (W)
spectral filter	2 mm of Cu
detector: Varex 2315N CMOS Flat Panel X-ray Detector	
pixel size	74.8 µm
field of view	
pixel	3072 × 1944
area	229.8 mm × 145.4 mm
max. frame rate (unbinned)	26 fps
dynamic range	14 bit
imaging geometry	
source-detector distance D	308 mm
source-sample distance R	55 mm to 155 mm
magnification m	5.6 to 2.0
data acquisition	
projections N	1440
exposure time	0.5 s to 1.0 s
max. volume (voxels)	3072 × 3072 × 1944
voxel size (cubic)	13.4 µm to 37.6 µm
sample size (cylinder H/W)	200 mm/100 mm
compute ressources	
disk storage	12 × 1.92 TB SSD Raid
linux compute server	DELL PowerEdge R7525
CPU	AMD EPYC 7282 2.80 GHz
GPU	NVIDIA A100 40 GB
RAM	512 GB

After each campaign, the data is transferred to DESY's dCache for longterm storage of the raw data. Reconstructions are published in the Research Data Repository (RDR) of the University of Hamburg [17].

Experimental procedures

The stringent requirements on the weight restricted the X-ray optical design, leading to a very compact and highly conical imaging geometry. The source to detector distance is 308 mm as compared to an active area of the detector of 229.8 mm × 145.4 mm. This imaging geometry is very sensitive to the geometric details of the setup, requiring careful calibration after assembly. Besides the typical acquisition parameters such as the number of projections, angular range, and exposure time, the tomographic reconstruction requires the precise knowledge of a set of reconstruction parameters accurately defining the specific imaging geometry. The latter is depicted schematically in Fig. 2, showing the seven free parameters that need to be determined to fully represent it in the tomographic model.

Following the calibration procedure described in [18], we make two rotation scans of a calibration sample made of a small metallic sphere (see Fig. 2 for a schematic). In between the two scans, we move the object a defined distance along the $\vec{e}_z$ direction. In the two separate scans, the sphere traces out two ellipses on the detector that are automatically fitted. From these ellipses, the geometry parameters are calculated analytically [18]. The most sensitive parameters are the rotation η that needs to be determined to better than 0.01 mrad and the horizontal positions u_0 and $\hat{u}$ of the detector surface normal pointing towards the source and the perpendicular projection of the origin O onto the detector that both need to be determined to within less than one pixel. The coordinates v_0 and $\hat{v}$ are less sensitive.

After calibration, the system is ready for tomographic data acquisition. ENCI can be operated in a wide range of experimental parameters, allowing tomographic imaging of a large variety of objects that fit into the scanner and are not too absorbing. In the following, we will restrict the discussion to the imaging of cuneiform tablets, i. e., clay objects that typically fit into the palm of a hand and are maximally 100 mm by 50 mm by 200 mm in size. Fig. 3 shows the linear attenuation coefficient for several types of clay. While the details of the attenuation below 70 keV are given by photo absorption and depend on the composition of the clay and in particular on the presence of heavier elements (such as iron in the case of the Illite [19]), the attenuation coefficient above this energy is dominated by Compton scattering and is thus nearly independent of the material composition and only weakly dependent on X-ray energy. To avoid strong beam hardening effects, it is thus advantageous to remove most of the spectrum below 70 keV, in particular since this lower part of the spectrum is strongly attenuated by a typical clay tablet. This can be achieved by introducing a copper filter of 2 mm thickness at the X-ray source.

Its effect is illustrated in Fig. 4. Fig. 4a shows the unfiltered model spectrum (W target, 180 keV) together with the spectrum that is transmitted through a 4 cm thick piece of clay. The lower part of the transmission spectrum (< 70 keV) is almost completely absorbed by the clay and contributes very little to the transmission image. The transmission spectrum is strongly shifted towards high-energy X-rays, with its centre of mass above 100 keV. Fig. 4b shows a tomographic slice through a replica of a cuneiform tablet without spectral filtering, exhibiting a strong distortion of the reconstructed effective attenuation coefficient. Fig. 4c depicts the relative attenuation values on the horizontal section through the slice shown in Fig. 4b. Compared to that at the outer rim of the object, the attenuation in its central part is underestimated by almost a factor two. Fig. 4d shows the smaller spectral shift of the filtered spectrum. In this case, the main part of the spectrum lies well above 70 keV, where the energy dependence of the attenuation coefficient of clay is small (see Fig. 3). As a result, the beam hardening is rather weak, as shown in Fig. 4e, with a maximal variation in reconstructed attenuation of about 10 %. The reconstructed values for the effective attenuation coefficient lie in the range of 0.3 cm^{-1} which coincides with the almost constant attenuation coefficient above 100 keV in Fig. 3. As a result of this choice of parameters, the reconstructed effective attenuation is quantitative within 10 %.

The rather homogeneous reconstruction of the attenuation of the clay makes the further image processing steps much easier and more reliable, allowing a systematic rendering of the surfaces (see Sec. Visualisation of high-resolution computed tomography data).

For most of the tablets, the tomographic data acquisition is therefore done with an acceleration voltage of 170 kV to 180 kV, an X-ray tube current of 100 µA to 200 µA, leading to an exposure time between 1.0 s and 0.5 s to fully utilise the dynamic range of the detector, respectively.

After centring the tablet on the rotary stage and ensuring it is within the field of view at the given magnification from all perspectives, N projection images are acquired over a full rotation (360°). Rotation at constant angular velocity avoids the time overhead of step scanning, resulting in complete acquisition in typically less than 13 min (170 kV, 200 µA).

Tomographic parameters and reconstruction

In practice, $N = 1440$ have been proven to be a good number of projections, as a further increase of N does not result in an improvement of the 3D image quality. Before and after the scan, a series of flat-field images are taken (without the object in the beam). Similarly, dark-field images (with X-rays turned off) are recorded to account for the noise background of the detector. All data are stored in HDF5 files using the NeXus standard for tomography [22].

After dark- and flat-field correction, the negative logarithm of the projections is fed into a Feldkamp algorithm [23] with generalised cone beam projections implemented in the ASTRA Toolbox [24]. The tomographic reconstruction of the full volume takes less than 15 min on the on-board Linux server. After reconstruction, the effective attenuation is sampled on a Cartesian 3D grid of cubic voxels. The voxel size is set to d_{det}/m, where d_{det} is the detector pixel size and m is the magnification defined by the ratio of source to detector and source to rotation axis distances $m = D/R$ (see Fig. 2). The full volume comprises $3072 \times 3072 \times 1944$ voxels, equivalent to approximately 73 GB of single-precision floating-point data.

For the tomographic reconstructions presented here, a spatial resolution of approximately 65 µm ± 10 µm (half pitch) was achieved, as determined by Fourier-ring correlation analysis [25]. Here, the resolution is primarily limited by photon noise due to the rapid tomographic scanning. In theory, ENCI can deliver tomographic reconstruction results with spatial resolutions of approximately 15 µm to 40 µm (half pitch), depending on the specific imaging geometry and magnification. As described in Sec. Experimental procedures, beam-hardening effects were significantly reduced by spectral filtering, which reduced density variations to below 10 %. Therefore, no additional numerical corrections were required to compensate for beam hardening in this case. Some example slices through the 3D tomographic data volume of different tablets are shown in Figs. 5a, 7b, and 9a,c,d. However, reading the text on the enclosed tablets requires further analysis and visualisation.

Visualisation of high-resolution computed tomography data

The next step is to extract the surfaces of different parts of an encased cuneiform tablet from the tomographic 3D volume data in order to be able to visualise these surfaces in 3D. Specialised tools for cuneiform inscriptions like GigaMesh [7] lack this geometric extraction of the surfaces, and generic data processing tools like Avizo [26] or VTK [27] do not support automatic extraction, segmentation, and interactive visualisation of separated artefact parts, inscriptions, and other features of interest. Existing processing tools require time-consuming manual processing of the volume data [11] and are not very responsive for the large data volumes at hand.

To address these shortcomings and to provide the desired features, we developed and implemented software tools to automate the extraction of geometric data from the reconstructed volume data. This includes separating the tablet and the envelope, detecting features, and providing interactive visualisation. Figs. 5a,b show a single slice through the CT volume data and the final 3D visualisation, respectively. This is achieved by batch-oriented processing to convert the CT volume data into feature-enriched geometry data representing clay surfaces. The extracted surfaces can then be interactively visualised for the Assyriologist to analyse the resulting tablets, their envelopes, and possible inclusions, e. g., of organic material.

Figs. 5c,d illustrate the intermediate steps of the data processing pipeline, which consists of three main components: 1. preprocessing of volume data, 2. extraction, and 3. postprocessing of surface data. For fast and efficient processing we utilise multi-threading (OpenMP [28]) and vectorisation (SIMD [29]), to exploit multi-level parallelism provided by modern workstations, and to enable near-real-time processing on site, where in general no access to cloud or high-performance computing services exists.

In the following, the main steps of our 3D data visualisation pipeline will be outlined (see Fig. 5).

The preprocessing stage uses a series of filters to process the volume data (Fig. 5c), modifying it on the regular 3D grid to reduce noise and enhance the desired characteristics. We use a low-pass filter combined with 2:1 sampling, followed by iterative bilateral filtering [30], which reduces the noise, while preserving the sharp transitions between clay and air [Fig. 5c(ii)].

To reconstruct the surfaces at the boundary of clay to air, we implemented an advanced isosurface algorithm. It delivers a triangular representation of a surface in 3D that approximates points in a volume that have the same given threshold (isovalue). Here, a suitable isovalue lies between the effective attenuation values of clay and air [gray area in Fig. 5c(iii)]. To facilitate the selection of an appropriate isovalue, we developed and implemented an automatic isovalue detection algorithm that analyses the probability distribution of the attenuation values and calculates the optimal isovalue. For the subsequent isosurface extraction, we implemented an advanced table-based 2-manifold dual marching cubes algorithm [31–33], which creates triangles at the location of the thresholded voxels [Fig. 5c(iv)].

In the postprocessing stage, extracted surfaces which are represented as a triangular mesh are smoothed to reduce small irregularities while preserving significant

features, such as high curvatures at the wedges of cuneiform symbols, taking advantage of iterative median or bilateral filtering of face normals, and adapting vertex positions [Fig. 5c(v)].

This leaves the components of the mesh corresponding to the tablet, envelope, and inclusions unidentified. Inclusions are conventionally identified as small, closed objects without connectivity with either the envelope or the tablet, thereby permitting to assign them to a distinct category. The shape and orientation can be analysed using eigenvalue decomposition of the covariance tensor of their mesh, enabling anisotropy-based classification and PCA-based size and alignment estimation [34, 35]. Figs. 9a,b illustrate this characterisation for what appears to be an enclosed seed.

Conversely, the tablet and the envelope may touch in certain areas, causing them to form a single, connected mesh. These areas are typically characterised by high negative curvature (concavity) around their borders. In order to delaminate the tablet and envelope at these junctions, we developed a segmentation approach based on local mesh curvature. Fig. 5d illustrates the separation process at locations where the curvature surpasses a predefined threshold. This results in the tablet and envelope being segmented and later identified as separate partitions.

To enhance the visual effects, shape features based on the two principal curvatures at each vertex of the mesh are extracted. These features accentuate cuneiform symbols by darkening and lightening areas of concave and convex shape, respectively. A further per-vertex attribute representing ambient light occlusion is precalculated, resulting in a more realistic symbol shading [Fig. 5b, Figs. 5c(vi-viii)].

The interactive visualisation application supports 3D presentation and interaction technologies, including (auto-)stereoscopic displays, as well as hand-tracking for gesture control. Previously extracted curvature and ambient occlusion attributes enhance the recognition of inscriptions, while colouring and the optional disabling of separate partitions aid visual exploration and scientific investigation of cuneiform tablets. The application also allows users to export open file formats, such as PLY and STL, for use with external graphics software or 3D printing. A detailed description of the processing and image analysis software can also be found in Olbrich et al. [36].

Results

ENCI on mission to Ankara

ENCI was deployed to the Museum of Anatolian Civilisations in Ankara for a period of three weeks, beginning in mid-September 2024. During this mission, 64 tomograms of 48 tablets and other objects were recorded, analysed and visualised. We present selected tablets from this mission that are sealed in their envelopes and preserved at the Museum of Anatolian Civilisations in Ankara.

Seeing through the envelope: A wife's hidden letter revealed

The envelope with its tablet inside, Kt 94/k 1150, was excavated in the house of Šalim-Aššur in the lower town of Kanesh. It dates back to the first half of the 19th century BCE. The envelope contains three lines of text on its obverse, and eight impressions of

the seal of Anna-anna, the wife of Ennum-Aššur, one of the two sons of Šalim-Aššur, on all sides [37, no. 298].

The text on the envelope reads as follows: "To Ennum-Aššur, son of Šalim-Aššur. Seal of Anna-anna". The woman Anna-anna has rolled her cylinder seal several times on the surface of the envelope, twice on the obverse and on the reverse, as well as on every edge (see Fig. 6a). The whole content of the letter addressed by Anna-anna to her husband is hidden. The text on the tablet was revealed after scanning the artefact with ENCI. Fig. 6b shows all the sides of the hidden tablet. The hidden letter can now be read and translated.[3]

[1-2]Say to Ennum-Aššur: thus (says) Anna-anna.
[3-4]According to the instructions you sent me, [5-6]regarding Laqēpum, I have been repeatedly going to him, and [7]he (always answered) as follows: [7-8]"I paid the silver to Kudātum."
[9-10]I checked and went to him (saying) as follows: [11-13]"I will certainly get witnesses (to testify) against you in case you did not pay (it) to Kudātum." [13-14]He (answered) as follows: [15]"I will not give the silver to you. [16-18]When Ennum-Aššur arrives, it will be to him that I will pay (it)!"
[18]You are my master. [19-20]Why do you keep turning your head towards the lapis lazuli?
[21-26]Here, your instructions concerning silver, 10 or 20 minas that are either in Burušhattum, or in Wahšušana, or here, you left your instructions [26-27]and you keep turning your head towards it. [28]If within 10 days you have not arrived, [29-30]as for your departure, stand up and come. [32]I hear bad words all the time!

This letter sent by a woman to her husband belongs to the archive excavated during the 1994 mission at Kültepe. Ennum-Aššur was a merchant travelling through different towns in Central Anatolia for his trading activities and asked his wife to get back some silver that he had lent to a colleague. The colleague refused to give back the silver to Anna-anna, explaining that he would only return the money to her husband on his return. It is an invaluable information about the status of women in this society of merchants involved in long-distance trade. Often alone and at the head of their households, these women also intervened in their husbands' business affairs [38].

A letter containing two pages

One of the letter envelopes, also excavated during the 1994 mission at Kültepe, has a protrusion on its obverse, suggesting the addition of a second small tablet inside (see Fig. 7a).

The tomographic reconstruction of the contents of this envelope confirmed this hypothesis as is visible in the tomographic slice (see Fig 7b) and the 3D rendering of the hidden inner two tablets (see Fig. 7c). If a letter writer filled the entire surface of the obverse, the lower edge, the reverse, the upper edge and finally the left edge of

[3]Transliteration of the letter : Tablet Kt 94/k 1150b, [1]*a-na En-um-A-šur* [2]*qí-bi-ma um-ma A-na-a-na-/ma* [3]*a-ma-lá té-er-tí-kà* [4]*ša ta-áš-pu-ra-ni* [5]*a-šu-mì Lá-qé-pì-im* [6]*a-ta-na-lá-ak-šu-ma* [7]*um-ma šu-ut-ma* kù-°babbar° [8]*a-na Ku-da-tim áš-qul* [9]*áš-ni-ma a-li-ik-šu-ma* [10]*um-ma a-na-ku-ma* [11]*ší-bi*$_4$: *lá-áš-ku-na-ku-um* lo.e.[12]*a-šar a-na Ku-da-tim* [13]*lá ta-áš-qú-lu um-ma* °ku° [14]°x x° *šu-ut-ma* rev.[15]kù-babbar *ku-a-tí lá a-da-na-ki-/im* [16]*i-na a-lá-ak* [17]*En-um-A-šur šu-a-tí-ma* [18]*a-ša-qál be-lí a-ta* [19]*mì-nam ur-ki*$^{!}$(SÁ) *hu-sá-ri-im* [20]*qá-qá-ad-kà ta-ta-na-i* [21]*a-na-kam té-er-ta-kà* [22]kù-babbar 10 *ma-na ù* 20 *ma-na* [23]*lu i-na Bu-ru-uš-ha-tim* [24]*lu i-na Wa-ah-šu-ša-na* [25]*lu a-na-kam té-er-ta-* °*kà*° u.e.[26]*té-zi-ib qá-qá-ad/-kà* [27]*ta-ta-na-i* l.e.[28]*šu-ma a-dí* 10 *u*$_4$*-me lá ta-/li-kam* [29]*a-ṣí-kà*? *té-eb-a-/ma* [30]*a-tal-kam* : [31] « *a-ta-kam* »[32]*a-wa-tim lá-am-na-tim áš-ta-na-/me-e*

the clay tablet, but had not finished delivering their message, they could still shape a second, smaller, flat, oval tablet on which they could add up to a dozen lines on the obverse [39]. This phenomenon is attested only in the Assyrian archives unearthed at Kanesh.

Several of these small oval tablets have been found, but there is generally nothing to link them to the main tablet once the envelope has been opened in antiquity. The additional tablet, designated as such in Old Assyrian (*ṣibat ṭuppim*), bears the cuneiform signs of the main tablet in negative on its reverse, which has made virtual separation of the two tablets particularly difficult. By visualising the two hidden tablets, it was possible to determine that the second tablet was placed on the obverse of the first and following the same orientation (see Fig. 7c). The envelope was shaped over the two tablets and the text written on it perpendicular to the text on the tablets, the obverse of the envelope covers the reverse of the main tablet.

The translation of the main and supplementary tablet reads:[4]

> [1-4]Say to the creditor and Elālī; say to the creditor: thus (says) Inba-Aššur.
> [5-10]5 minus 1/4 *kutānum*-textiles of good quality, 10 textiles either from Akkad or from Harahur, 2 black donkeys, I am bringing you all this. [11-13]I gave 10 textiles extra for the transport costs until Hahhum. [14-15]Send me the silver of the consignment by the next caravan. [15-16]Send me (also) small goods worth 5 shekels of silver. [17-19]Before being in Hahhum, the day Ennum-Aššur came down, [19-20]my goods came out of the palace. [20-21]During two days my donkeys suffered, so [22-23]I will drive them to Timilkiya. You are my brother, [24]let your report come to me.
> Supplementary tablet: [1-3]Take a decision concerning the excellent quality textiles, take a decision concerning your textiles.

The writer announces the arrival of a consignment of textiles from southern Mesopotamia and Assur on two donkeys, and asks his correspondents to sell the merchandise and return the proceeds in the form of silver. He stopped in Hahhum, a town located at the crossing of the Euphrates, halfway between Assur and Kanesh. The text on the additional tablet is not clearly linked to that on the main tablet.

Cancellation of a contract

Another encased letter, Kt 93/k 144, was discovered in the house of Ali-ahum and his son Aššur-taklāku during the 1993 excavation campaign in Kültepe.

The text revealed on the tablet describes the procedure to be followed with the encased contract in the time of loan repayment. The text written on the envelope is perpendicular to the one on the tablet, and the obverse of the envelope covers the

[4]Transliteration of the letter: Tablet Kt 94/k 602b, [1]*a-na* dam-gàr$^{ri\text{-}im}$ *ù* [2]*E-lá-lí* : *qí-bi-ma* [3]*a-na* dam-gàr$^{ri\text{-}im}$ *qí-bi-ma* [4]*um-ma In-ba-A-šùr-ma* [5]5 *lá* 1/4$^{?}$ túg *ku-ta-ni* sig$_5$ [6]10 túg *lu ša A-ki-dí-e* [7]*lu ša Ha-ra-hu-ur* [8]2 anše *ṣa-lá-mu* [9]*mì-ma a-nim* lo.e.[10]*a-ra-dí-a-kum* rev.[11]10 túg *wa-at-ru-ma* [12]*a-na ta-ší-a-tí-im* [13]*a-dí Ha-hi-im* : *a-dí-in* [14]kù-babbar *ša šé-bu-lim* : *a-na* [15]*pá-ni-a* : *šé-bi$_4$-lam ṣa-he-er-/tám* [16]*ša* 5 gín kù-babbar *šé-bi$_4$-lam* [17]°*lá*°*-ma* : *i-na Ha-hi-im* [18]*i-na* ^{d}utu^{i} *En-um-A-šùr* [19]*ur-da-ni* : *ú-nu-tí i-na* [20]é-gal^{lim} : *ú-ṣa-am* : 2 u_4*-me-/e* [21]*e-ma-ru-a* : *i-nu-hu-ma* u.e.[22]*a-na Tí-mì-il$_5$-ki-a* [23]*a-sá-ri-dam* : *a-hi a-ta* le.e.[24]*té-er-ta-kà* : *a-pá-ni-a* [25]*li-li-kam*, supplementary tablet: [1]túg^{hi}*-tù* sig$_5$ diri [2]*mì-lik* : túg^{hi}*-tí-kà* [3]*mì-lik*. Line 7, the toponym Harahur is also attested in KTS 2, 30:4.

reverse of the tablet. The hidden letter can now be read and translated as follows (see Fig. 8):[5]

> [1-5]Thus (say) Ali-ahum and Aššur-taklāku: say to Iddin-abum, Ennānum, Puzur-Aššur and Ikuppiya.
> [5-6]There, I have seen the tablets, and [7-11]the enveloped tablet concerning 5 minas of silver that Aššur-ṭāb gave as investment loan to Ikuppīya and [12]that the creditor had written down, [13-14]give him the tablet so that he cancels it (kills it). [14-17]Here, I wrote the tablet of his joint stock company with his investors.

When the creditor grants a loan, the contract is written on a tablet. This tablet is then wrapped in a clay envelope, and the text of the contract is repeated or summarised on the envelope, to which the witnesses and the debtor have rolled their seals. When the debt is repaid, the creditor gives the document to the debtor, who cancels it by breaking the envelope. Ali-ahum is literate since he explains at the end of his letter that he wrote another partnership contract.

This written artefact is not only interesting for its textual content, but also for the inclusions in the clay discovered by X-ray tomography as will be shown in the next section.

Inclusions in the clay

Depending on how carefully the clay was prepared, it could contain various inclusions. To obtain a fine, pure clay, decantation or levigation was used to separate the coarse elements from the fine ones by grinding and dispersing them in water [40]. The letters written by the Assyrian merchants used a coarse clay, full of mineral and bio-organic inclusions. The tomographic section of this encased tablet, Kt 93/k 144, shows an object trapped in a layer of the envelope, which appears to be a seed (see Figs. 9a,b).

This seed has been identified by Andrew Fairbairn, the archaeobotanist working at the excavation site in Kültepe. According to him "This is a barley seed, clearly visible in the overall shape with the chisel like ends, dorsiventrally flattened shape and shallow ventral furrow. It is probably hulled barley." Barley was widely cultivated in the whole South Western Asia.

In most cases, the tablet and its envelope were made from the same clay, with a similar density of inclusions. However, in rare instances, such as Kt 91/k 287, excavated in 1991 in the house of Elamma, the clay is completely different (see Fig. 9c). This suggests that the tablet was first made, and much later on, and presumably at another location, it was wrapped in a clay envelope. The text on the envelope indicates that the tablet contains a sworn testimony by Laqepum about a confrontation between Pilah-Aššur and Elamma [41, no. 104]. The text ends at the left-hand edge, indicating that Laqepum gave this tablet at the Gate of the God. Perhaps the tablet was encased there a few days after it was written.

---

[5]Transliteration of the letter: Tablet Kt 93/k 144, [1]*um-ma A-lá-hu-um-ma* [2]*ù A-šùr-ták-lá-ku* [3]*a-na I-dí-a-bi-im En-na-/nim* [4]*Puzur$_4$-A-šùr ù I-ku-/pì-a* [5]*qí-bí-ma : a-ma-kam* [6]*ṭup-pé-e : am-ra-ma* [7]*ṭup-pá-am ha-ar-ma-/am* [8]*ša* 5 *ma-na* kù-babbar [9]*ša a-na I-ku-pí-a* lo.e.[10]*a-na e-bu-ṭí* rev.[11]*A-šùr-*dù$_{10}$ *i-dí-nu-ma* [12]dam-gàr *il$_5$-pu-tù* [13]*ṭup-pá-am dí-na-šu-ma* [14]*li-du-uk : a-na-kam* [15]*ṭup-pu-um ša na-ru-qí-/šu* [16]*iš-tí : um-mì-a-ni-šu* [17]*al-pu-ut.*

Shaping envelopes

In general, the envelope was made when the tablet was at least partially dry, so that the clay of the envelope would not stick to the clay on the tablet. If a caravan was about to leave Assur while the tablet was being written, it would then be protected by a thin textile before the envelope was made, as can be seen from the textile impressions on the surface of some tablets.

A preliminary study based on the analysis of the inner surfaces of clay envelope fragments discovered at Kültepe in 1993 proposed a reconstruction of how the envelopes were manufactured. To make the envelope, the clay has to be rolled or stretched out as though it were pastry for a pie. The entire surface of the tablet is then covered and the envelope is closed by superimposing two layers of clay over one side of the tablet. Experiments carried out at the time showed that achieving a very thin layer of clay was relatively difficult, suggesting that the envelope was made with a single layer of clay [2].

However, tomographic sections of the encased tablets show that envelopes are systematically multilayered: An envelope is made by folding the clay over several times (see the tomographic section shown in Fig. 9d). It is highly likely that multiplying the layers of clay to form an envelope made it more solid, particularly for transport. Additionally, the air trapped between the layers of clay may help the envelope to dry without cracking. Further experimentation is required to confirm these observations and reconsider the method of making clay envelopes.

Discussion

The use of the ENCI transportable tomographic scanner on dozens of cuneiform tablets in their clay envelopes has produced results far beyond what it was originally designed for. We can now access the hidden text of the cuneiform tablets, determine how carefully the clay in the tablets and envelopes was prepared, and analyse the techniques used to make the tablets and their clay envelopes. ENCI has also been tested on other cultural heritage artefacts such as a Georgian codex from the ninth century CE, whose cover is made up of several layers of ancient manuscripts glued together, Egyptian statuettes and Mesopotamian cylinder seals. The very high resolution and portability of the instrument means that all kinds of ancient artefacts can now be analysed without damage.

Data availability

Photos, tomographic volume data, and 3D geometry files of the different investigated cuneiform tablets can be found at:

Kt 91/k 287: https://doi.org/10.25592/uhhfdm.17632
Kt 93/k 144: https://doi.org/10.25592/uhhfdm.17634
Kt 93/k 550: https://doi.org/10.25592/uhhfdm.17636
Kt 94/k 602: https://doi.org/10.25592/uhhfdm.17638
Kt 94/k 1150: https://doi.org/10.25592/uhhfdm.17640

The unprocessed tomographic raw data can be obtained from the authors upon reasonable request.

Code availability

Our data processing code is based on Python and utilises the ASTRA Toolbox for the tomographic reconstruction in cone-beam geometry [24]. It is available upon request. Our visualisation software EXAVIS42 is publicly available [42].

References

[1] Béranger, M.: Fonctions et usages des enveloppes de lettres dans la Mésopotamie des IIIe et IIe mil. av. J.-C. (2340-1595 av. J.-C.). Épistolaires **44**, 25–43 (2018)

[2] Michel, C.: Making clay envelopes in the Old Assyrian period. In: Kulakoğlu, F., Michel, C., Öztürk, G. (eds.) Integrative Approaches to the Archaeology and History of Kültepe-Kanesh, Kültepe, 4-7 August, 2017, Kültepe International Meetings 3, SUBARTU XLV, pp. 187–203. Turnhout, Brepols (2020). https://shs.hal.science/halshs-02996202/

[3] The Electronic Text Corpus of Sumerian Literature: T2.1.4, Sargon and Ur-Zababa. https://etcsl.orinst.ox.ac.uk/cgi-bin/etcsl.cgi?text=t.2.1.4#

[4] Spataro, M., Taylor, J., O'Flynn, D.: A technological study of Assyrian clay tablets from Nineveh, Tell Halaf and Nimrud: a pilot case study. Archaeological and Anthropological Sciences **15**(5), 68 (2023) https://doi.org/10.1007/s12520-023-01761-0

[5] Project RFA09: Reading Closed Cuneiform Tablets Using High-resolution Computed Tomography, Within the Frame of the Deutsche Forschungsgemeinschaft – EXC 2176 'Understanding Written Artefacts: Material, Interaction and Transmission in Manuscript Cultures', Project No. 390893796. https://www.csmc.uni-hamburg.de/research/cluster-projects/field-a/rfa09.html

[6] Anderson, S.E., Levoy, M.: Unwrapping and visualizing cuneiform tablets. IEEE Computer Graphics and Applications **22**, 82–88 (2002) https://doi.org/10.1109/MCG.2002.1046632

[7] Mara, H., Krömker, S., Jakob, S., Breuckmann, B.: GigaMesh and Gilgamesh 3D multiscale integral invariant cuneiform character extraction. In: The 11th International Symposium on Virtual Reality, Archaeology and Cultural Heritage VAST, pp. 131–138 (2010). https://doi.org/10.2312/VAST/VAST10/131-138

[8] Fisseler, D., Müller, G.G.W., Weichert, F.: Web-Based Scientific Exploration and Analysis of 3D Scanned Cuneiform Datasets for Collaborative Research. Informatics **4**, 44 (2017) https://doi.org/10.3390/informatics4040044

[9] Diara, F., Barsacchi, F.G., Martino, S.d.: Moving beyond the Content: 3D Scanning and Post-Processing Analysis of the Cuneiform Tablets of the Turin Collection. Applied Sciences **14**(11), 4492 (2024) https://doi.org/10.3390/app14114492

[10] NINO Leiden: Seeing Through Clay: 4000 Year Old Tablets in Hypermodern CT Scanner. https://www.nino-leiden.nl/message/seeing-through-clay-4000-year-old-tablets-in-hypermodern-ct-scanner

[11] Wassink, J.: Cuneiform in a Scanner. https://www.tudelft.nl/en/delft-outlook/articles/cuneiform-in-a-scanner/

[12] Juliš, K., Kumpová, I., Mynářová, J., Pech, M., Polák, L., Štefcová, P., Valach, J., Vavřík, D., Wolf, B., Zemánek, P.: Memory Tools. National Museum, Prague (2020)

[13] Bossema, F.G., Palenstijn, W.J., Heginbotham, A., Corona, M., van Leeuwen, T., van Liere, R., Dorscheid, J., O'Flynn, D., Dyer, J., Hermens, E., Batenburg, K.J.: Enabling 3D CT-scanning of cultural heritage objects using only in-house 2D X-ray equipment in museums. Nature Communications **15**, 3939 (2024) https://doi.org/10.1038/s41467-024-48102-w

[14] Baker Hughes Company: Phoenix Nanotom M (2021). https://www.bakerhughes.com/sites/bakerhughes/files/2024-10/bhcs38584_phoenix_nanotom_m_brochure_r2_1.pdf

[15] Group, T.: TESCAN micro-CT solutions. https://info.tescan.com/micro-ct

[16] Mkrtchyan, T., Chitrapu, K., Garonne, V., Litvintsev, D., Meyer, S., Millar, P., Morschel, L., Rossi, A., Sahakyan, M.: dcache: Inter-disciplinary storage system. EPJ Web of Conferences **251**, 02010 (2021) https://doi.org/10.1051/epjconf/202125102010

[17] https://www.fdr.uni-hamburg.de

[18] Noo, F., Clackdoyle, R., Mennessier, C., White, T.A., Roney, T.J.: Analytic method based on identification of ellipse parameters for scanner calibration in cone-beam tomography. Physics in Medicine & Biology **45**(11), 3489–3508 (2000) https://doi.org/10.1088/0031-9155/45/11/327

[19] Ajouyed, O., Hurel, C., Marmier, N.: Evaluation of the Adsorption of Hexavalent Chromium on Kaolinite and Illite. Journal of Environmental Protection **02**(10), 1347–1352 (2011) https://doi.org/10.4236/jep.2011.210155

[20] Schoonjans, T., Brunetti, A., Golosio, B., Sanchez del Rio, M., Solé, V.A., Ferrero, C., Vincze, L.: The xraylib library for x-ray–matter interactions. recent developments. Spectrochimica Acta Part B: Atomic Spectroscopy **66**(11), 776–784 (2011) https://doi.org/10.1016/j.sab.2011.09.011

[21] Poludniowski, G., Omar, A., Bujila, R., Andreo, P.: Technical note: Spekpy v2.0—a software toolkit for modeling x-ray tube spectra. Medical Physics **48**, 3630–3637 (2021) https://doi.org/10.1002/mp.14945

[22] Könnecke, M., Akeroyd, F.A., Bernstein, H.J., S.Brewster, A., Campbell, S.I., Clausen, B., Cottrell, S., Hoffmann, J.U., Jemian, P.R., Männicke, D., Osborn, R., Peterson, P.F., Richter, T., Suzuki, J., Watts, B., Wintersberger, E., Wuttke, J.: The NeXus data format. Applied Crystallography **48**, 301–305 (2014) https://doi.org/10.1107/S16005767140275

[23] Feldkamp, L.A., Davis, L.C., Kress, J.W.: Practical cone-beam algorithm. J. Opt. Soc. Am. A **1**(6), 612–619 (1984) https://doi.org/10.1364/JOSAA.1.000612

[24] Aarle, W.v., Palenstijn, W.J., Cant, J., Janssens, E., Bleichrodt, F., Dabravolski, A., Beenhouwer, J.D., Batenburg, K.J., Sijbers, J.: Fast and flexible X-ray tomography using the ASTRA toolbox. Optics Express **24**(22), 25129 (2016) https://doi.org/10.1364/oe.24.025129

[25] Heel, M., Schatz, M.: Fourier shell correlation threshold criteria. Journal of Structural Biology **151**(3), 250–262 (2005) https://doi.org/10.1016/j.jsb.2005.05.009

[26] Avizo Software: Materials Characterization Software. https://www.thermofisher.com/de/de/home/electron-microscopy/products/software-em-3d-vis/avizo-software.html

[27] Schroeder, W.J., Martin, K., Lorensen, W.E.: The Visualization Toolkit: An Object-Oriented Approach To 3D Graphics. Kitware, Inc., Clifton Park, NY (2018)

[28] OpenMP Application Programming Interface. OpenMP Architecture Review Board (2015)

[29] Furht, B.: Simd (single instruction multiple data processing). In: Encyclopedia of Multimedia, pp. 817–819. Springer, Boston, MA (2008)

[30] Durand, F., Dorsey, J.: Fast bilateral filtering for the display of high-dynamic-range images. In: Proceedings of the 29th Annual Conference on Computer Graphics and Interactive Techniques, pp. 257–266 (2002). https://doi.org/10.1145/566654.566574

[31] Lorensen, W.E., Cline, H.E.: Marching cubes: A high resolution 3D surface construction algorithm. In: Proceedings of the 14th Annual Conference on Computer Graphics and Interactive Techniques - SIGGRAPH '87, vol. 21, pp. 163–169. ACM Press, New York, NY (1987). https://doi.org/10.1145/37402.37422

[32] Schaefer, S., Warren, J.: Dual marching cubes: primal contouring of dual grids.

In: 12th Pacific Conference on Computer Graphics and Applications, pp. 70–76 (2004). https://doi.org/10.1109/PCCGA.2004.1348336

[33] Grosso, R., Zint, D.: A parallel dual marching cubes approach to quad only surface reconstruction. Vis Comput **38**, 1301–1316 (2022) https://doi.org/10.1007/s00371-021-02139-w

[34] Westin, C.-F., Maier, S.E., Khidhir, B., Everett, P., Jolesz, F.A., Kikinis, R.: Image processing for diffusion tensor magnetic resonance imaging. In: Taylor, C., Colchester, A. (eds.) Medical Image Computing and Computer-Assisted Intervention – MICCAI'99, pp. 441–452. Springer, Berlin, Heidelberg (1999). https://doi.org/10.1007/10704282_48

[35] Kindlmann, G.: Superquadric tensor glyphs. In: Deussen, O., Hansen, C., Keim, D.A., Saupe, D. (eds.) Joint EUROGRAPHICS - IEEE TCVG Symposium on Visualization (2004). https://doi.org/10.2312/VisSym/VisSym04/147-154

[36] Olbrich, S., Beckert, A., Michel, C., Schroer, C., Ehteram, S., Schropp, A., Paetzold, P.: Efficient analysis and visualization of high-resolution computed tomography data for the exploration of enclosed cuneiform tablets. In: 14th Symposium on Large Data Analysis and Visualization (LDAV) (2024). https://doi.org/10.1109/ldav64567.2024.00012

[37] Larsen, M.T.: The Archive of the Šalim-Aššur Family, Vol 1: The First Two Generations, Kültepe Tabletleri 6a. Türk Tarih Kurumu Yayınları 6/33d-a, Ankara (2010)

[38] Michel, C.: Women of Aššur and Kaneš: Texts from the Archives of Assyrian Merchants, Writings from the Ancient World vol. 42. SBL, Atlanta (2020)

[39] Michel, C.: Binding cuneiform tablets in one unit. In: Bausi, A., Friedrich, M. (eds.) Tied and Bound, Studies in Manuscript Cultures, vol. 33, pp. 11–37. De Gruyter, Berlin (2023). https://www.degruyter.com/document/doi/10.1515/9783111292069-002/html

[40] Taylor, J., Cartwright, C.: The making and remaking of clay tablets. Scienze dell' Antichita **17**, 297–324 (2011)

[41] Veenhof, K.R.: Kültepe Tabletleri VIII: The Archive of Elamma, Son of Iddin-Suen, and His Family (Kt. 91/k 285-568 and Kt. 92/k 94-187). Türk Tarih Kurumu Yayınları. VI. Dizi, vol. Sayı 33f. Türk Tarih Kurumu, Ankara (2017)

[42] Olbrich, S., Beckert, A.: EXAVIS42 – Efficient methods for creation, feature extraction, and interactive visualization of isosurfaces of 3D volume data (2024). https://doi.org/10.25592/uhhfdm.16616 . https://www.fdr.uni-hamburg.de/record/16616

Fig. 1 **a** Schematic drawing of the modular design. The eight components are 1) tomographic scanner base, 2) sample chamber, 3) slider for the X-ray tube, 4) X-ray tube including high-voltage generator, 5) and 6) are shielding for the X-ray tube, and 7) is the detector including the backside of the sample chamber, 8) the server rack. **b** Tomographic scanner ENCI at the Museum of Anatolian Civilisations in Ankara, Türkiye. **c** Front view of the scanner with the sample chamber open and a cuneiform tablet mounted.

Fig. 2 Generalised cone beam geometry. For the definition of the seven free parameters, we follow the definitions in [18].

Fig. 3 Linear attenuation coefficient calculated for two exemplary clay minerals, i. e., Kaolinite and Illite as described in [19]. Coming from a natural source, the Illite composition here is considered to give a realistic estimate of potential contaminations of natural clays. The density was assumed to be 2.65 g cm^{-3} and 2.75 g cm^{-3}, respectively. Attenuation coefficients were calculated using "xraylib" [20].

Fig. 4 **a-c** Beam hardening for the unfiltered spectrum of a tungsten X-ray tube operated at 180 kV. **a** Modelled spectrum (blue) of the X-ray tube and the attenuated spectrum (green) behind 40 mm of Kaolinite (rescaled by 10×). **b** Tomographic reconstruction of an enclosed cuneiform tablet (replica) recorded in ENCI without filter at 180 kV. **c** Effective attenuation coefficient on the blue section in Fig. **b**. Beam hardening leads to a strong distortion of the effective attenuation coefficient. **d** Modelled spectrum (light blue) of the X-ray tube behind a 2 mm copper filter and the attenuated spectrum (green) behind 40 mm of Kaolinite (rescaled by 10×). **e** Tomographic reconstruction of the enclosed cuneiform tablet (replica) recorded in ENCI with 2 mm copper filter at 180 kV. **f** Effective attenuation coefficient on the blue section in Fig. **e**. Its value corresponds well with the almost constant attenuation coefficient above 100 keV in Fig. 3. The spectra in **a** and **d** were modelled using "s pekPy" [21].

Fig. 5 **a** Grayscale visualisation of density data measured by CT, sliced orthogonally to x-axis (dark grey: clay, light grey: plastic holder, white: air). **b** Visualisation of surfaces of the extracted envelope (cut, brown), tablet (ochre), and inclusions (semitransparent, light grey) of tablet Kt 94/k 1150a. **c** Steps of data processing and visualisation pipeline. Voxel and tablet surface representations, and its 3D renderings are based on a cutout in Fig. **b**. **c**(i) Original voxel data slice from CT, **c**(ii) denoised voxel data slice, **c**(iii) thresholded voxel data slice, **c**(iv) triangulated surface with wire frame and thresholded voxel data, **c**(v) smoothed surface with wire frame and thresholded voxel data, **c**(vi) flat shading of surface, based on directed light, **c**(vii) smooth shading (Phong) of surface, and **c**(viii) combined with shape and ambient-occlusion-based darkening and highlighting. **d** 2D illustration of the process of separating the envelope from the tablet. **d**(i) Horizontal 2D slice of CT data. **d**(ii) Extraction of isosurfaces (dark grey line) and detection of high curvature points. **d**(iii) Disconnected surfaces at high curvature points result in separated tablet (ochre) and envelope (brown).

Fig. 6 **a** Envelope of the letter (Kt 94/k 1150a). Museum of Anatolian Civlisations, Ankara. Size of the envelope: 5.3 cm × 4.9 cm × 2.6 cm. Photos: Samaneh Ehteram. **b** Visualisation of the hidden tablet (Kt 94/k 1150a). White surface coloring emphasises estimated patches where the envelope touches the tablet. Bounding box: 46.5 mm × 50.3 mm × 17.3 mm.

Fig. 7 **a** Photo of the upper edge of the envelope of Kt 94/k 602a. Museum of Anatolian Civilisations, Ankara. Photo: Cécile Michel. This unopened envelope has the following dimensions: 5.5 cm × 5.2 cm × 3.1 cm. The tomographic section **b** shows the two tablets inside the envelope; the bright objects inside the clay are tiny stones. **c** 3D visualisation of the two hidden tablets, Kt 94/k 602b (main tablet) and Kt 94/k 602c (small extra tablet), shows how the additional small tablet was placed on the main tablet. Left side: both the main tablet and its small extension tablet as they are assembled within the envelope, middle: observe sides, and right: reverse sides of both tablets, respectively.

Fig. 8 **a** Photo of the envelope Kt 93/k 144a (obverse). Museum of Anatolian Civilisations, Ankara. Photo: Cécile Michel. **b**, **c** 3D visualisations of the envelope and the encased tablet, respectively. The tablet (obverse) is rotated by 90° as compared to the envelope for better readability of the cuneiform text. Different colors in **b** indicate different segmented areas. Size of the envelope: 5.3 cm × 4.8 cm × 2.9 cm.

Fig. 9 **a** Tomographic section through the tablet Kt 93/k 144, showing the large inclusion as a void in the clay. **b** Visualisation of inclusions (semitransparent, one emphasised in yellow) within the envelope (brown, semitransparent, cut) of Kt 93/k 144 (tablet coloured in ochre). The large object seems to be a seed. Annotated size is derived from the PCA-aligned bounding box of the surface mesh vertices. **c** The tomographic section of Kt 91/k 287 shows that the clay of the tablet, which has many inclusions, is completely different from the clay of the envelope. **d** The tomographic section of Kt 93/k 550 shows that the envelope is multilayered.

Acknowledgements

The research for this project was funded by the Deutsche Forschungsgemeinschaft (DFG, German Research Foundation) under Germany´s Excellence Strategy – EXC 2176 "Understanding Written Artefacts: Material, Interaction and Transmission in Manuscript Cultures", project no. 390893796. The research was conducted within the scope of the Centre for the Study of Manuscript Cultures (CSMC) at Universität Hamburg. Thanks to the successive spokespersons of the Excellence Cluster, Michael Friedrich and Konrad Hirschler who have supported our project from the very start. We would like to acknowledge the support of Mirko Pollok and Silvio Achilles in developing the tomographic reconstruction software and the detector integration. Simone Starlinger, Jan Horstmann, and Juliane Wilke in engineering and construction, the DESY Central Mechanics Group for preparing the production drawings, the DESY workshops for the challenging production of the very complex mechanical components, in particular Markus Kowalski and Dmitrij Seibel fabricating the radiation protection assemblies. Julia Müller from the DESY Central Electronics Group for her advice and support with the CE and X-ray certification of the device. Leila Mokhtari Oranj and Anne Wefer made a detailed modelling for the radiation protection and provided radiation safety advice. For the study mission at the Louvre Museum, we thank Ariane Thomas, head of the Department of Oriental Antiquities, Mahmoud Alassi, for his help for the logistics, and Véronique Pataï, who supported us throughout our stay and provided us with the cuneiform tablets. For the study mission at the Museum of Anatolian Civilisations, we also wish to thank Yusuf Kıraç, the Museum Director, and Umut Alagöz, the Vice-Director who welcomed the team and ENCI, as well as the staff of the tablet section, Mine Çifçi, İsmet Aykut, Başak Demiryurek, and Sevda Metin. Our warmest thanks to Fikri Kulakoğlu, Professor of archaeology and Director of Kültepe excavations and Tunç Sipahi, Head of the department of Archaeology, Protohistory and Archaeology of Asia Minor of Ankara University who have supported our project. We would also like to express our gratitude to Sophie Gauthier, former director of the French Institute in Ankara, for her help, and warmly thank Andrew Fairbairn who identified for us the seed inclusion in Kt 93/k 144.

Author contributions

The project was conceived and led by C.M. and C.G.S., who combined their expertise in Assyriology and X-ray science. Project leads are C.M., C.G.S., and S.O. C.G.S. and A.S. developed the X-ray physical concept of the mobile CT scanner. C.G.S. and P.P. developed the workflows for calibration and tomographic reconstruction. S.O. and A.B. developed the surface extraction and visualisation software. R.D., P.W., S.B.,

and M.B. developed the full engineering concept, detailed technical design, system monitoring and controls and the assembly of the ENCI device including documentation and certification. C.M, C.G.S., A.S., S.E., P.P., K.Z., and A.A. were part of the experimental mission to the Museum of Anatolian Cultures in Ankara, involved in data acquisition, tomographic reconstruction, segmentation, and visualisation. C.M. read, transliterated and translated the Old Assyrian texts on the cuneiform tablets and envelopes and analysed the materiality of the written artefacts. C.M., C.G.S. and S.O. wrote the manuscript. C.M., A.S. and C.G.S. reviewed and edited the manuscript. C.M., C.G.S., P.P., A.S., A.B., and S.O. made the figures. All authors reviewed and commented on the manuscript.

Competing interests

The authors have no competing interests as defined by Springer, or other interests that might be perceived to influence the results and/or discussion reported in this paper.

Correspondence. Correspondence and requests for materials should be addressed to Cécile Michel, Andreas Schropp, and Christian G. Schroer.

Peer review information.

Open Access.

a

b

c

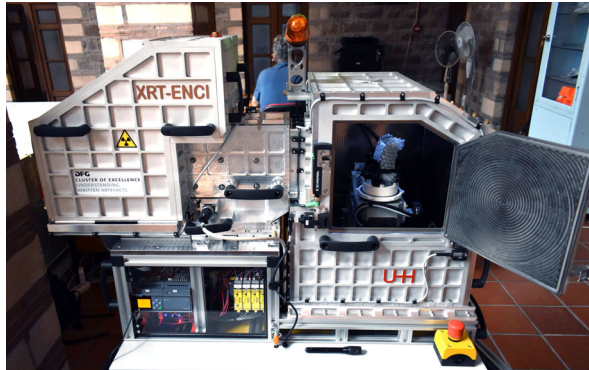

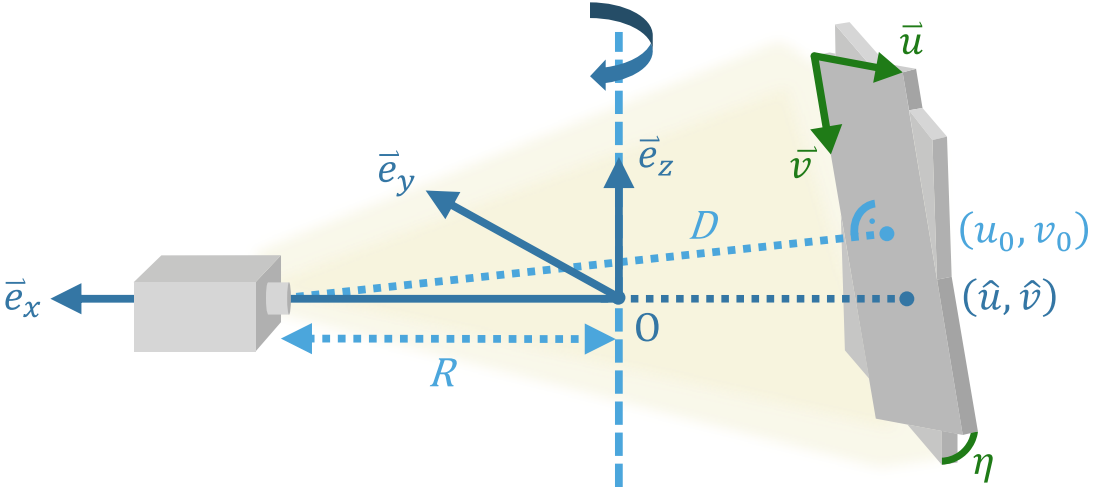

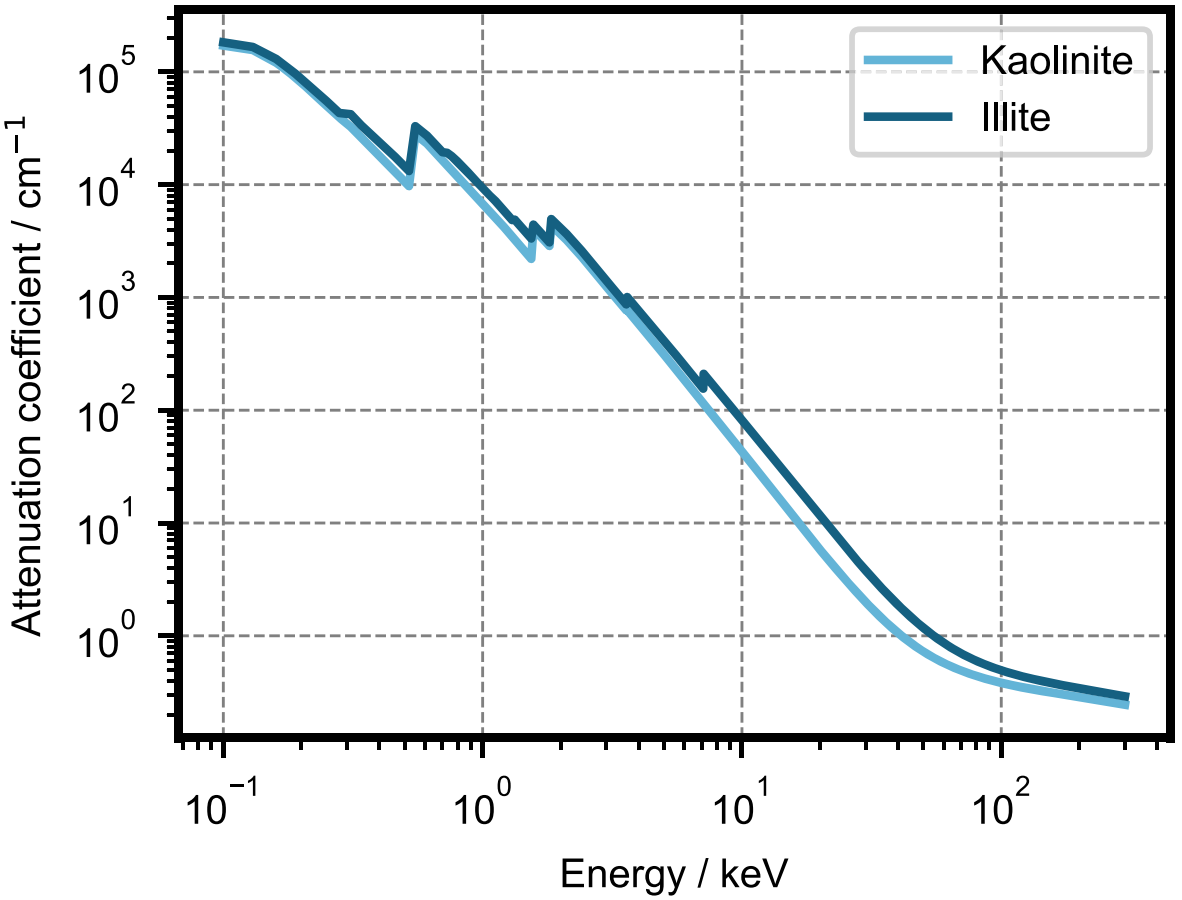

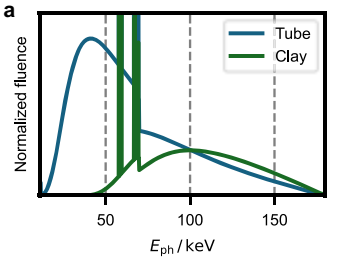
a
Normalized fluence
Tube
Clay
50
100
150
E_{ph} / keV

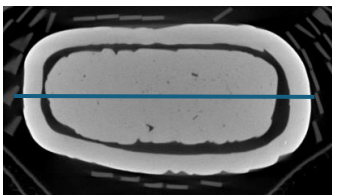
b

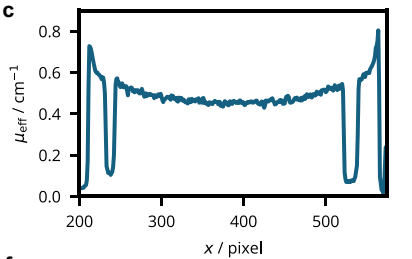
c
μ_{eff} / cm^{-1}
0.0
0.2
0.4
0.6
0.8
200
300
400
500
x / pixel

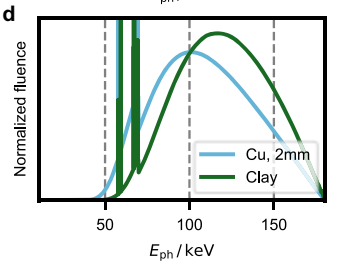
d
Normalized fluence
Cu, 2mm
Clay
50
100
150
E_{ph} / keV

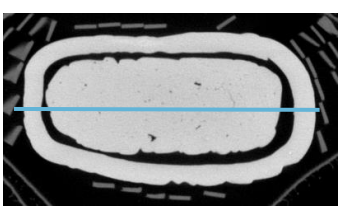
e

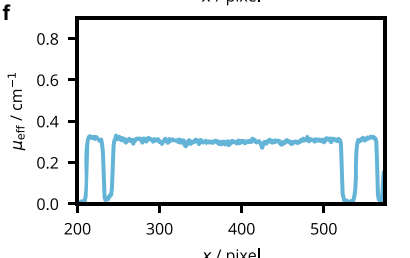
f
μ_{eff} / cm^{-1}
0.0
0.2
0.4
0.6
0.8
200
300
400
500
x / pixel

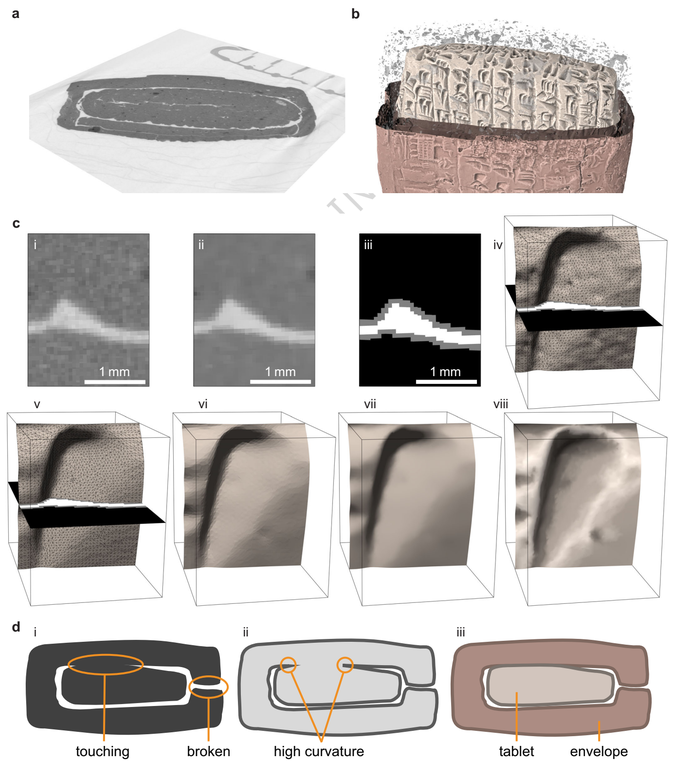
a
b
c
i
ii
iii
iv
1 mm
1 mm
1 mm
v
vi
vii
viii
d
i
ii
iii
touching
broken
high curvature
tablet
envelope

a

b

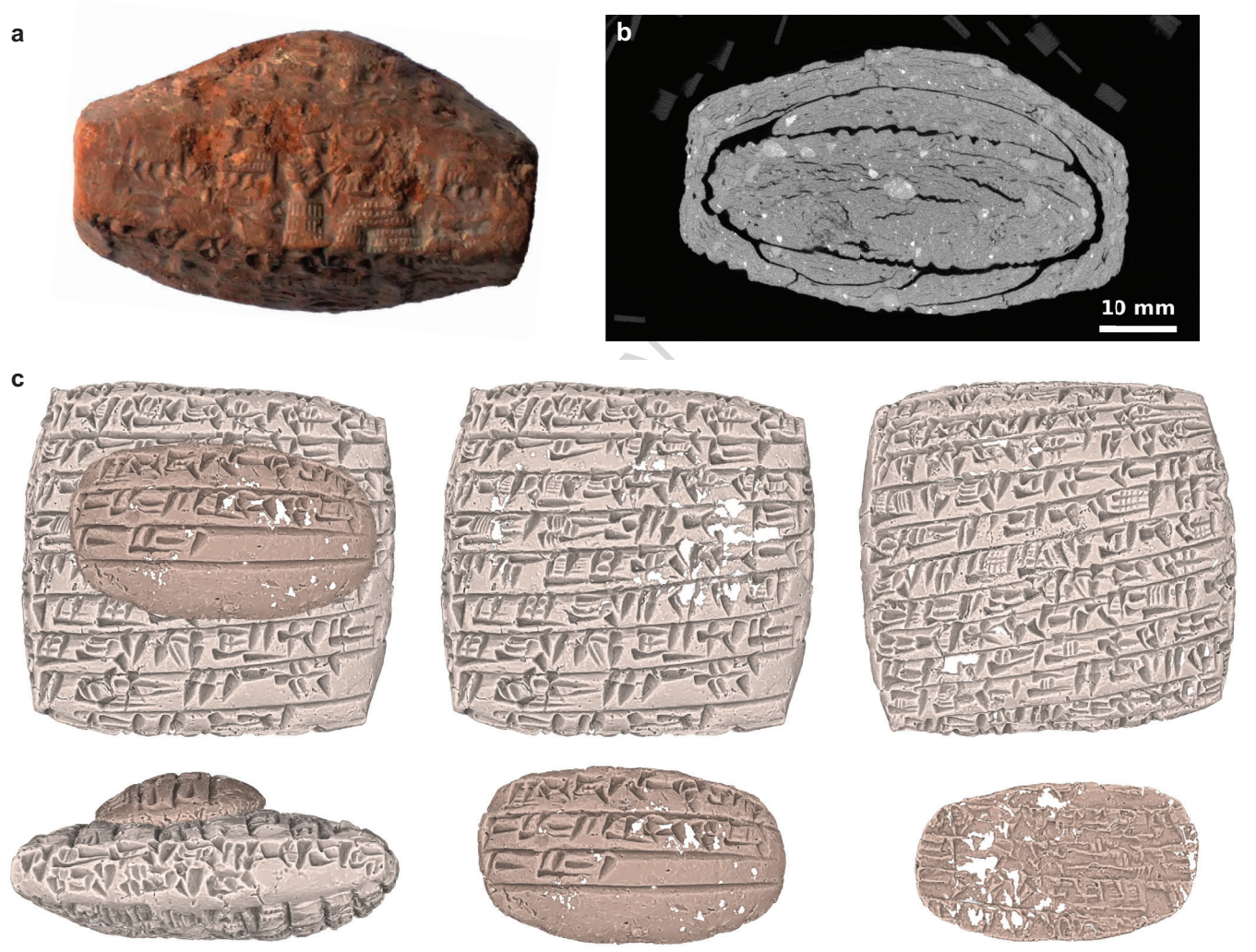
a
b
10 mm
c

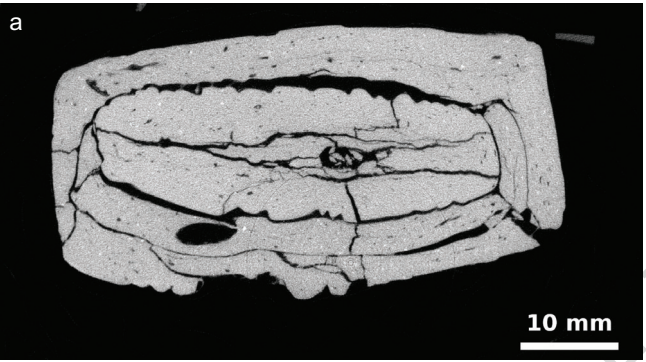
a
10 mm

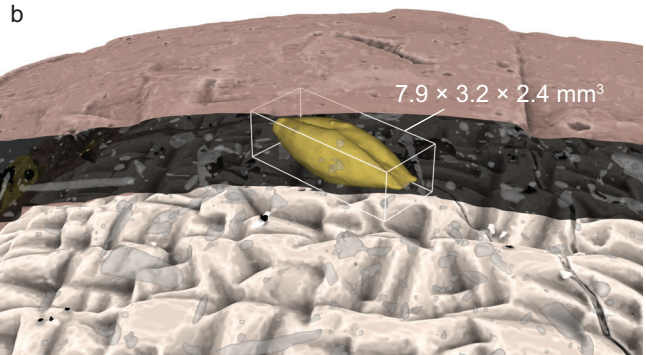
b
7.9 × 3.2 × 2.4 mm³

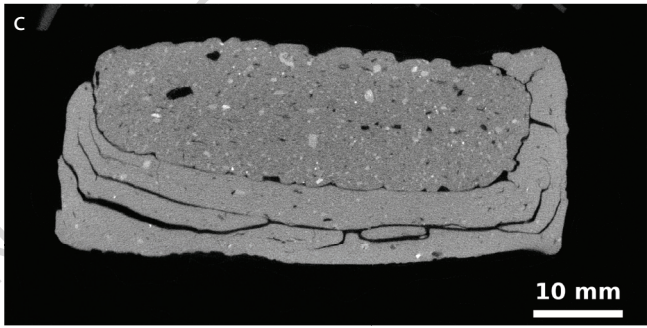
c
10 mm

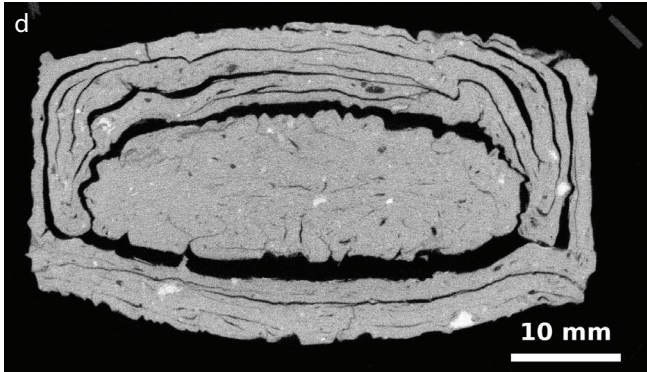
d
10 mm